J. Fluid Mech. (1982), *vol.* 117, *pp.* 123–142
Printed in Great Britain

Spatial and temporal characteristics of modulated waves in the circular Couette system

By M. GORMAN† AND HARRY L. SWINNEY
Department of Physics, The University of Texas, Austin, Texas 78712

(Received 5 February 1981 and in revised form 23 July 1981)

We have used flow-visualization and spectral techniques to study the spatial and temporal properties of the flow that precedes the onset of weak turbulence in a fluid contained between concentric cylinders with the inner cylinder rotating (the circular Couette system). The first three flow regimes encountered as the Reynolds number is increased from zero are well-known – Couette flow, Taylor-vortex flow, and wavy-vortex flow. The present study concerns the doubly periodic regime that follows the (singly periodic) wavy-vortex-flow regime. Wavy-vortex flow is characterized by a single frequency f_1, which is the frequency of travelling azimuthal waves passing a point of observation in the laboratory. The doubly periodic regime was discovered in studies of power spectra several years ago, but the fluid motion corresponding to the second frequency f_2 was not identified. We have found that f_2 corresponds to a modulation of the azimuthal waves; the modulation can be observed visually as a periodic flattening of the wavy-vortex outflow boundaries. Moreover, in addition to the previously observed doubly periodic flow state, we have discovered 11 more doubly periodic flow states. Each state can be labelled with two integers m and k, which are simply related to physical characteristics of the flow: m is the number of azimuthal waves, and k is related to the phase angle between the modulation of successive azimuthal waves by $\Delta\phi = 2\pi k/m$. This expression for the phase angle was first conjectured from the flow-visualization measurements and then tested to an accuracy of $0{\cdot}01\pi$ in spectral measurements. Recently Rand (1981) has used dynamical-systems concepts and symmetry considerations to derive predictions about the space–time symmetry of doubly periodic flows in circularly symmetric systems. He predicted that only flows with certain space–time symmetries should be allowed. The observed flow states are in agreement with this theory.

1. Introduction

A fluid contained between concentric cylinders with the inner cylinder rotating and the outer cylinder fixed (the circular Couette geometry) is one of a number of hydrodynamic systems which exhibit a sequence of distinct time-independent and time-dependent flow regimes that precede the transition to weak turbulence. The final preturbulent-flow regime in the circular Couette system that we have studied is characterized by power spectra that consist of two instrumentally sharp components and their integer-linear combinations. The onset of weak turbulence in this system is marked by the appearance of a broad spectral component in addition to the

† Present address: Department of Physics, University of Houston, Houston, TX 77004.

sharp frequency components of the doubly periodic regime. Just beyond the onset of weak turbulence the integrated spectral energy of the broad component is much less that the energy of the sharp components, and the turbulent intensity is small.

The power spectra and flow photographs for weakly turbulent flow in the Couette system differ only slightly from the spectra and photographs obtained for the final preturbulent flow. Hence it is reasonable to expect that the onset of turbulence will be easier to understand for such a flow than for flows such as plane Poiseuille flow in which the initial turbulent flow is quite different from the laminar flow which precedes it.

The idea that weakly turbulent flows can be described by only a few degrees of freedom was first discussed by Lorenz (1963*a*, *b*) and Ruelle & Takens (1971). In the past few years a number of investigators have found chaotic behaviour in models with a small number of nonlinear coupled ordinary differential equations. Although the models have been found to display a variety of types of dynamical behaviour, no realistic model of a real weakly turbulent flow has so far been obtained.

The selection of the appropriate modes for models with a finite number of modes will be greatly aided by the knowledge of the spatial and temporal characteristics of the preturbulent flows. The present work describes these characteristics for the final preturbulent flow in a system that exhibits weak turbulence.

In § 2 we define the system parameters and briefly review relevant past experiments, and in § 3 we describe our experimental methods. The experimental results are presented in § 4 and are compared with the theory of Rand (1981) in § 5. The work is discussed in § 6.

2. Background

Flows between concentric cylinders with the outer cylinder at rest are characterized by the following parameters: the radius ratio $\eta = a/b$, where a and b are respectively the inner and outer radii of the annulus; the Reynolds number $R = a\Omega(b-a)/\nu$, where Ω is the angular velocity of the inner cylinder and ν is the kinematic viscosity; the aspect ratio $\Gamma = h/(b-a)$, where h is the height of the annulus; and the boundary conditions (either fixed or free) at the ends of the annulus.

Most of our experiments discussed in this paper were conducted on a system with $\eta = 0{\cdot}883$ and $\Gamma = 20$; these parameters are typical of those used in many previous studies. For other η and Γ the sequence of transitions can be quite different from that discussed below.

The following sequence of regimes has been observed for $\eta = 0{\cdot}883$ and $\Gamma = 20$ (see DiPrima & Swinney 1981). At sufficiently small R the flow is nearly azimuthal except near the ends of the annulus; the flow between infinitely long cylinders would be purely azimuthal. For R above a critical value R_c, the azimuthal flow is unstable and a new flow, *Taylor-vortex flow* (TVF), develops (Taylor 1923). In TVF, toroidal vortices encircle the inner cylinder and are stacked in the axial direction. For $R/R_c > 1{\cdot}2$, travelling azimuthal waves form on the Taylor vortices. Coles (1965) found that the *wavy-vortex flow* (WVF) observed at a particular Reynolds number is not unique. In a system with $\Gamma = 27{\cdot}9$ he observed at some R as many as 25 different stable states characterized by different numbers of azimuthal waves m and axial vortices N. Velocity power spectra for WVF consist of a single frequency f_1 and its

harmonics; f_1 is found experimentally to equal the frequency with which the waves pass a point of observation in the laboratory.

Above $R/R_c = 10{\cdot}2$, Gollub & Swinney (1975) found that a second frequency appears in the velocity power spectra. Although these results were reproduced and extended in other laboratories (Walden & Donnelly 1979; Mobbs, Preston & Ozogan 1979; Bouabdallah & Cognet 1980), no other values of f_2 were reported nor was any information obtained about the fluid motion corresponding to f_2.† Using flow-visualization techniques, Gorman discovered the motion of the fluid which corresponds to f_2. Gorman & Swinney (1979) reported these characteristics of the mode f_2: the mode corresponds to both an amplitude and frequency modulation of the azimuthal waves; the magnitude of f_2 is different for different values of m; and for a given m there are multiple values of f_2 which correspond to different spatial characteristics of the modulation. The present paper reports a detailed flow-visualization and spectral study of the spatial and temporal characteristics of *modulated wavy-vortex flow* (MWVF).

The next transition that occurs at larger R/R_c is marked by the appearance of a broad frequency component f_B in the power spectrum. Thus the MWVF regime is the last preturbulent-flow regime (Fenstermacher, Swinney & Gollub 1979).

3. Experimental techniques

3.1 *The concentric-cylinder system*

The cylindrical annulus used in these experiments has inner and outer radii of 5·250 and 5·946 cm, respectively. The inner cylinder is brass with a black oxide coating, and the outer cylinder is precision-bore glass tubing. The lower horizontal fluid boundary is established by a Teflon ring attached to the outer cylinder, and the upper boundary is left free or is established by a ring similar to that at the lower boundary. Any aspect ratio from 0 to 44 can be selected by moving the upper ring. Most measurements were made with an aspect ratio of 20, thus largely avoiding (i) the end effects that occur in short annuli (see, for example, DiPrima & Swinney 1981, § 6.6; Benjamin 1978) and (ii) the dislocations that occur in long annuli (Donnelly *et al.* 1980).

3.2. *Flow-visualization measurements*

Flow patterns were rendered visible in water at room temperature using a suspension of small (about $5 \times 30\ \mu$m) platelets (Kalliroscope AQ1000) that align with the flow. In order to determine the time evolution of the wave pattern it was necessary to modify the apparatus used in a previous experiment (Gorman & Swinney 1979) so that the entire annulus could be viewed at all times. Two mirrors were used to obtain photographs of five overlapping images, each subtending about 110° azimuthal angle, as shown in figure 1. In figure 1 the direct view of the cylinder is labelled (1) and the four images are labelled (2)–(5), with the numbers increasing in the direction of the cylinder rotation. Figure 2 is a typical photograph obtained with the mirror arrangement shown in figure 1.

Still photographs and ciné films were made of each WVF and MWVF state that was

† The frequency f_2 was designated ω_3 by Gollub & Swinney (1975) and Fenstermacher, Swinney & Gollub (1979); they observed a transient component, designated ω_2, at lower R/R_c.

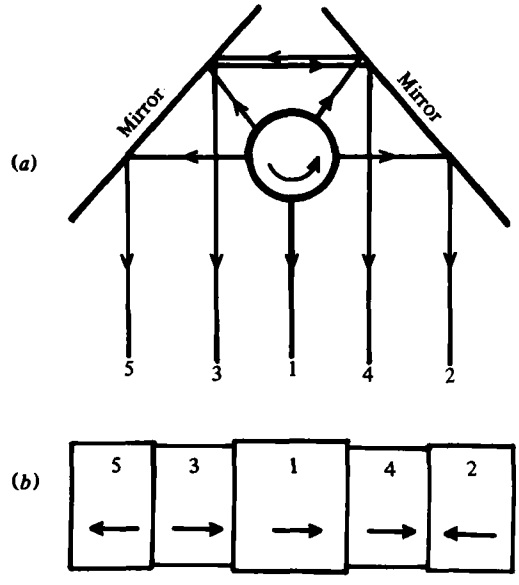

FIGURE 1. (a) The mirror arrangement for simultaneous observation of all the waves around the annulus. (b) The cylinder and its four images as seen by an observer in the laboratory; the arrows indicate the direction of the motion.

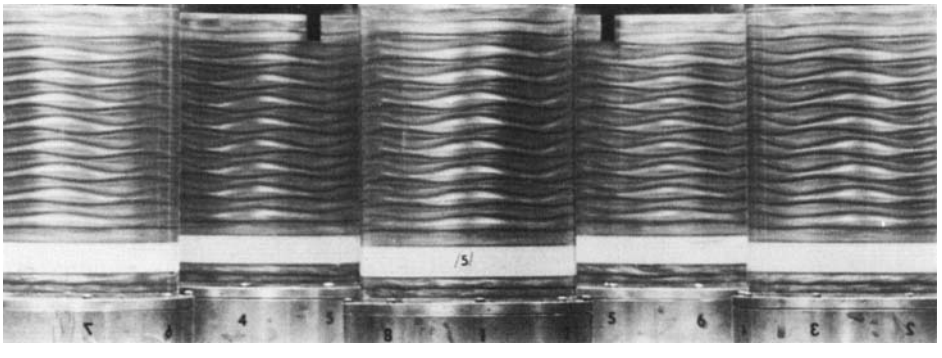

FIGURE 2. The complete wavy-vortex pattern for $m = 5$, photographed using the mirror arrangement diagrammed in figure 1.

observed. The still photographs were taken on Tri-X film with an Olympus OM-1 35 mm camera with 135 mm lens and a 2× teleconverter, and the prints were made on Ilfospeed 3·1 M RC paper. Ciné pictures were taken with a Kodak Special Reflex camera with a 50 mm lens on Tri-X reversal 7278 film shot at 24 frames/s with a 20 ms exposure time for each frame; in 20 ms at $R/R_c = 10$ the waves move about 0·1 cm in the azimuthal direction, which is much less than the azimuthal wavelength (8·8 cm for $m = 4$) or the axial wavelength (1·5 cm).

The time evolution of each wave was determined in a frame-by-frame analysis of the movie films. A LW International Photo Optical Data Analyzer Model 224A Special ciné projector, which can go forward or backward one frame at a time without loss of focus, was used to determine the film frame numbers at which each azimuthal

wave had successive modulation maxima – i.e. the frame numbers at which the vortex outflow boundary was the flattest.

3.3. *Power spectra*

Fenstermacher *et al.* (1979) used laser–Doppler velocimetry to measure the radial component of the fluid velocity. A disadvantage of the laser–Doppler technique is that the spatial character of the flow cannot be determined from these single-point measurements. The flow pattern cannot be simultaneously visualized because the scattering particles used in the Doppler velocity technique are small (typically 0·5 μm diameter) and isotropic, so the fluid appears homogeneous. We have not succeeded in making Doppler measurements with the platelets used in flow visualization.

We have made simultaneous spectral and flow-visualization measurements by measuring, instead of the velocity, another dynamical variable – the intensity of light scattered by the platelets used in flow visualization (Donnelly *et al.* 1980). The flow was seeded with platelets and illuminated with incoherent light. The scattered light was collected from a region equal to about one-quarter of the axial wavelength and was imaged on a photodiode. The photocurrent was digitized and recorded in the computer where the power spectrum was computed from time-series records of 1024 or 8192 points. The resultant spectra have the same features as those obtained from the laser measurements.

3.4. *Frequencies f_1, f_2, and f_2'*

The frequency f_1 is the frequency of the azimuthal waves passing a fixed point in the laboratory; f_2 is the frequency of modulation of these waves, as determined by an observer in the laboratory; and f_2' is the modulation frequency as determined by an observer fixed in a reference frame that rotates in phase with the azimuthal waves. In general, $f_2' \neq f_2$; however, there is a relationship between f_2 and f_2' which is discussed in § 4.2.

Values of f_1 and f_2 accurate to 0·3 % were obtained from power spectra, but f_1 and f_2 were also determined to within 1 % simply by using a stop-watch to determine by eye in real time or from movie films the time required for 20 waves or for 20 modulation cycles to pass the observer.

In WVF it is clear that the lowest-frequency component in the spectrum is the fundamental f_1. When a second fundamental frequency occurs in a power spectrum, it is not possible to identify which of the spectral components (that include fundamentals, harmonics, and combinations) correspond to the physical motion of the fluid, i.e. the modulation of the waves. Gollub & Swinney (1975) chose the most intense new spectral component as the second characteristic frequency; however, in our comparison of power spectra with visualization measurements it was found that in general f_2 was not the most intense new spectral component in MWVF. Thus the identification of f_2 in the spectrum was determined from the vizualization measurements.

In a reference frame that rotates in phase with the travelling azimuthal waves, an observer sees only one frequency f_2'. This frequency was determined from a frame-by-frame analysis of ciné films for each state of the flow. Each wave was followed through many successive oscillations (flattenings of the vortex outflow boundary) as the wave rotated around the annulus.

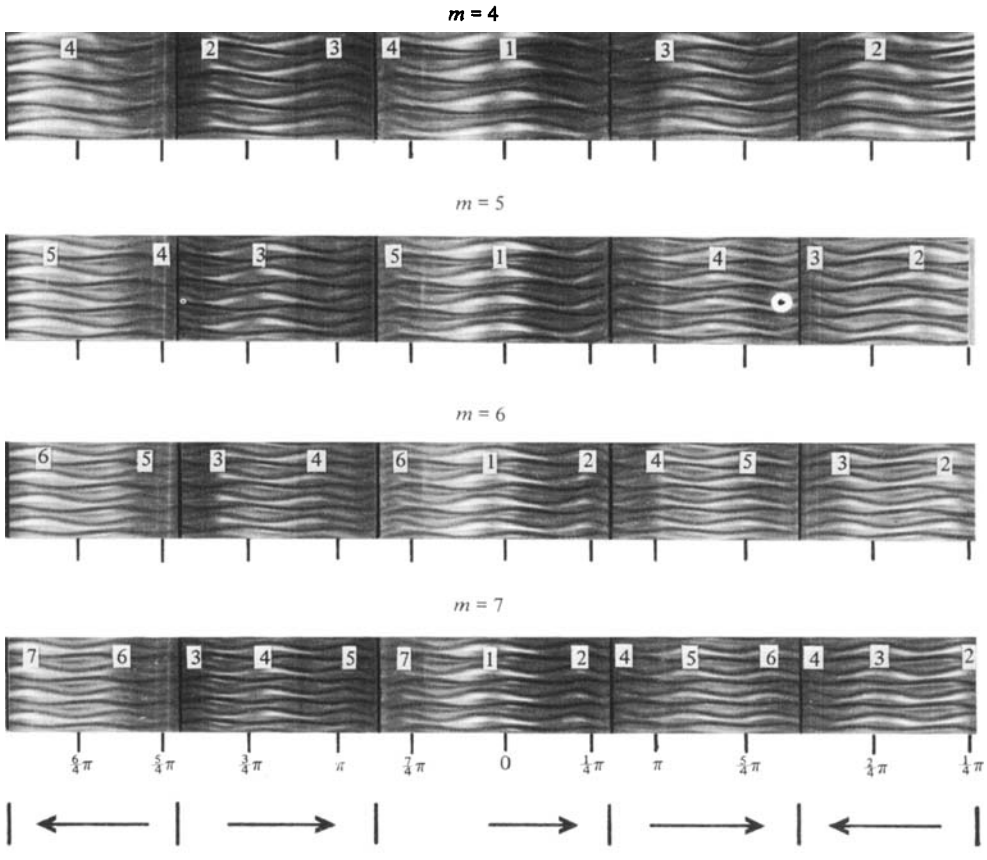

FIGURE 3. Wavy-vortex flow for $m = 4, 5, 6, 7$. Successive waves around the annulus in the direction of wave rotation are labelled 1, 2, ..., m.

4. Experimental results

Each different wave pattern that we have observed in doubly periodic MWVF will be shown in § 4.1 to be characterized by two integers m and k; hence the states will be labelled m/k. The frequencies that are characteristic of each state are described in § 4.2. Measurements of frequency modulation are described for two of the states in § 4.3. The procedure for producing each of the MWVF states is described in § 4.4.

4.1. *Wave patterns in doubly periodic MWVF*

In WVF the wave patterns have m-fold rotational symmetry. The vortex inflow and outflow boundaries are both S-shaped, as figure 3 illustrates for states with $m = 4$, 5, 6 and 7. The whole wave pattern rotates as a rigid body about the cylinder axis; hence the pattern is at rest for an observer fixed in a reference frame that rotates with the waves.

Beyond the onset of MWVF, a vortex outflow boundary, which is seen in the photographs as the darker of the two lines bordering a vortex, periodically oscillates from the S-shape shown in figure 3 to the flattened shape, as seen, for example, for the state labelled 5/0 in figure 4. In MWVF all the waves in the *axial* direction are

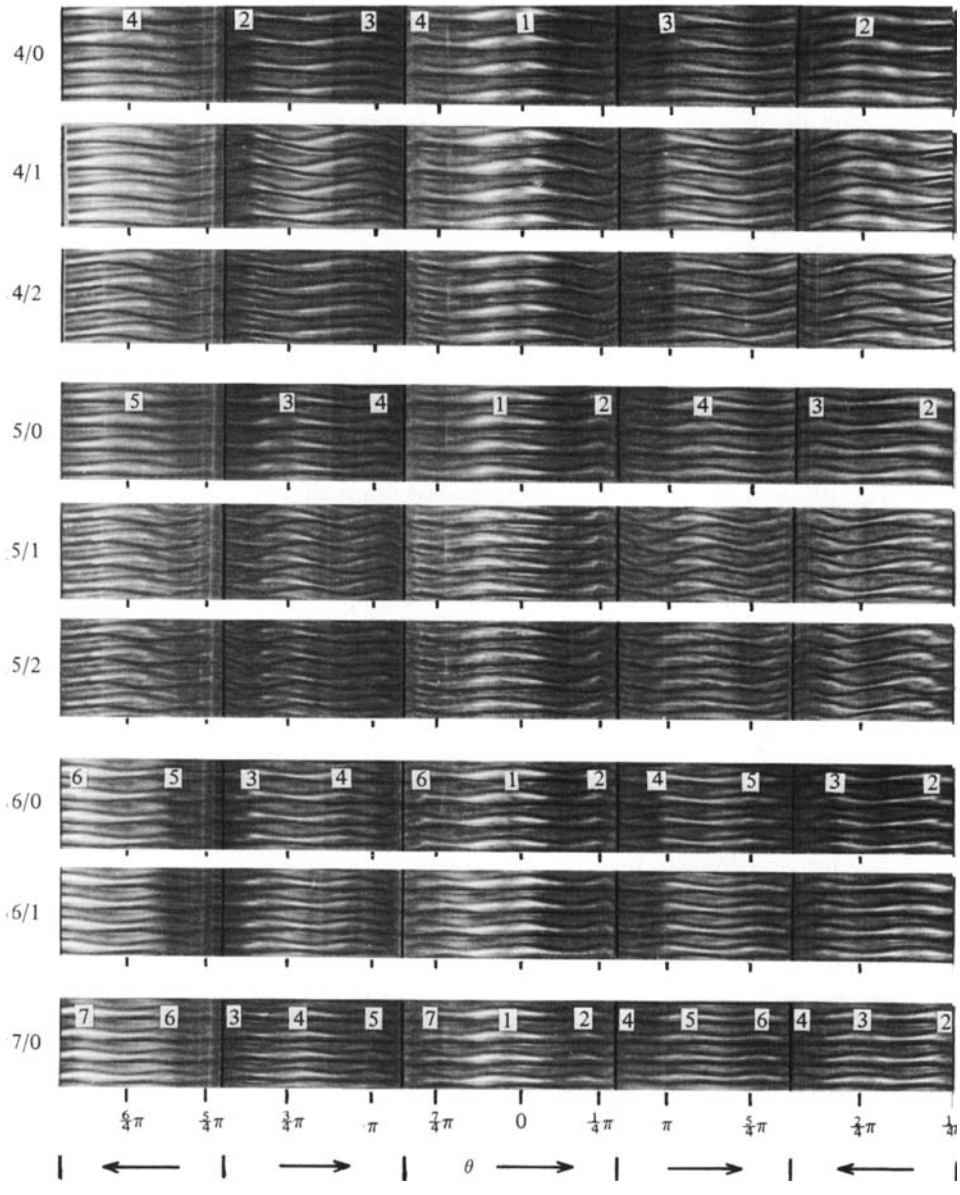

FIGURE 4. Photographs of nine of the observed modulated wavy-vortex flow states. Successive waves around the annulus in the direction of wave rotation are labelled 1, 2, ..., m. For each state at least one wave is flattened; it is labelled 1. For the $k = 0$ states all the waves are simultaneously modulated (flattened), as shown, while for the $k \neq 0$ states only the waves labelled 1 are completely flattened, except for the (2-fold symmetric) 4/2 state, where both waves (1) and (3) are completely flattened.

modulated in phase, while in the *azimuthal* direction the wave modulation can have the same phase, as in the 5/0 state in figure 4, or the modulation phase can vary with angle, as in the 5/1 state, where wave (1) is flattened and wave (3) is S-shaped.

We have determined the temporal evolution of the wave patterns for different MWVF states by analysing ciné film frame by frame. The five overlapping images of

the annulus in the ciné films made it possible to follow each individual wave as it rotated and its amplitude oscillated. For each of the m waves in a particular MWVF state the successive film frame numbers at which a wave flattened were measured, thus determining the relative phase of the modulation for each wave. This analysis showed that, for an observer fixed in a reference frame that rotates with the waves, the azimuthal and temporal dependence of the wave pattern can be described by a function of the form $a[2\pi f_2' t - \phi(\theta')]$, where f_2' is the frequency of oscillation of any point on the wave pattern and the temporal phase angle ϕ depends only on the azimuthal angle θ', which is measured with respect to the rotating frame and increases in the direction of cylinder rotation (Swift, Gorman & Swinney 1981). The *principal result of our experiments* is that the phase angle ϕ satisfies the simple expression

$$\phi(\theta' + 2\pi/m) = \phi(\theta') + 2\pi k/m, \tag{1}$$

where k is an integer.

This empirical equation was initially conjectured on the basis of an analysis of the ciné films. The phase difference $2\pi k/m$ determined from this analysis had an uncertainty of $0{\cdot}15\pi$. A more stringent test of this conjectured equation was then provided by an analysis of power spectra, as described by Swift *et al.* (1981); they show that a departure from (1) by only $0{\cdot}01\pi$ would produce spectral components that are absent from our spectra.

Equation (1) implies that for a given m there are only m distinct MWVF patterns. We have chosen k values from $-(\frac{1}{2}m-1)$ to $\frac{1}{2}m$ for even m, and k values from $-\frac{1}{2}(m-1)$ to $\frac{1}{2}(m-1)$ for odd m. The schematic diagrams in figure 5 show the temporal evolution of wave patterns for the states shown in figure 4. Each wave is represented by a sine function whose amplitude changes with time. The modulation is represented *schematically* as a uniform flattening of each wave, although alternative pictures of the modulation are possible (see § 6.1).

The enhanced horizontal lines indicate a maximum of the modulation, and their sequence can be used to specify each state. For states with $k = 0$ the vortex outflow boundaries of all waves simultaneously flatten, as figures 4 and 5 illustrate. For $k = 1$, successive waves are modulated in sequence; that is, waves (1), (2), ..., (m) successively flatten, as figure 5 illustrates for the 4/1, 5/1, and 6/1 states.

For the 4/2 state the modulation phase angle is π; hence the phase angle of the third wave relative to the first is 2π, so they flatten simultaneously, as shown in figure 4 and illustrated in figure 5. Waves (2) and (4) are modulated simultaneously, π out of phase with (1) and (3). For the 5/2 state the modulation phase angle is $\frac{4}{5}\pi$; the phase angles of waves (2) to (5) relative to wave (1) are: $0{\cdot}8\pi$, $1{\cdot}6\pi$, $2{\cdot}4\pi$ (or $0{\cdot}4\pi$), and $3{\cdot}2\pi$ (or $1{\cdot}2\pi$). Thus the sequence of wave flattenings is (1), (4), (2), (5), (3), as figure 5 illustrates.

Different starting procedures are used to produce different m/k states, as discussed in § 4.4. The characteristics of the twelve observed states are summarized in table 1; each of these states is stable indefinitely, once it is produced. It is probable that some of the predicted but unobserved m/k states are stable, but we have not yet found a way of producing them.

With the exception of the $m = 3$ state we have made ciné films and recorded power spectra for each of the observed states. Figures 4–7 illustrate this documentation for nine of the states; details will be discussed below. Now that a simple picture of

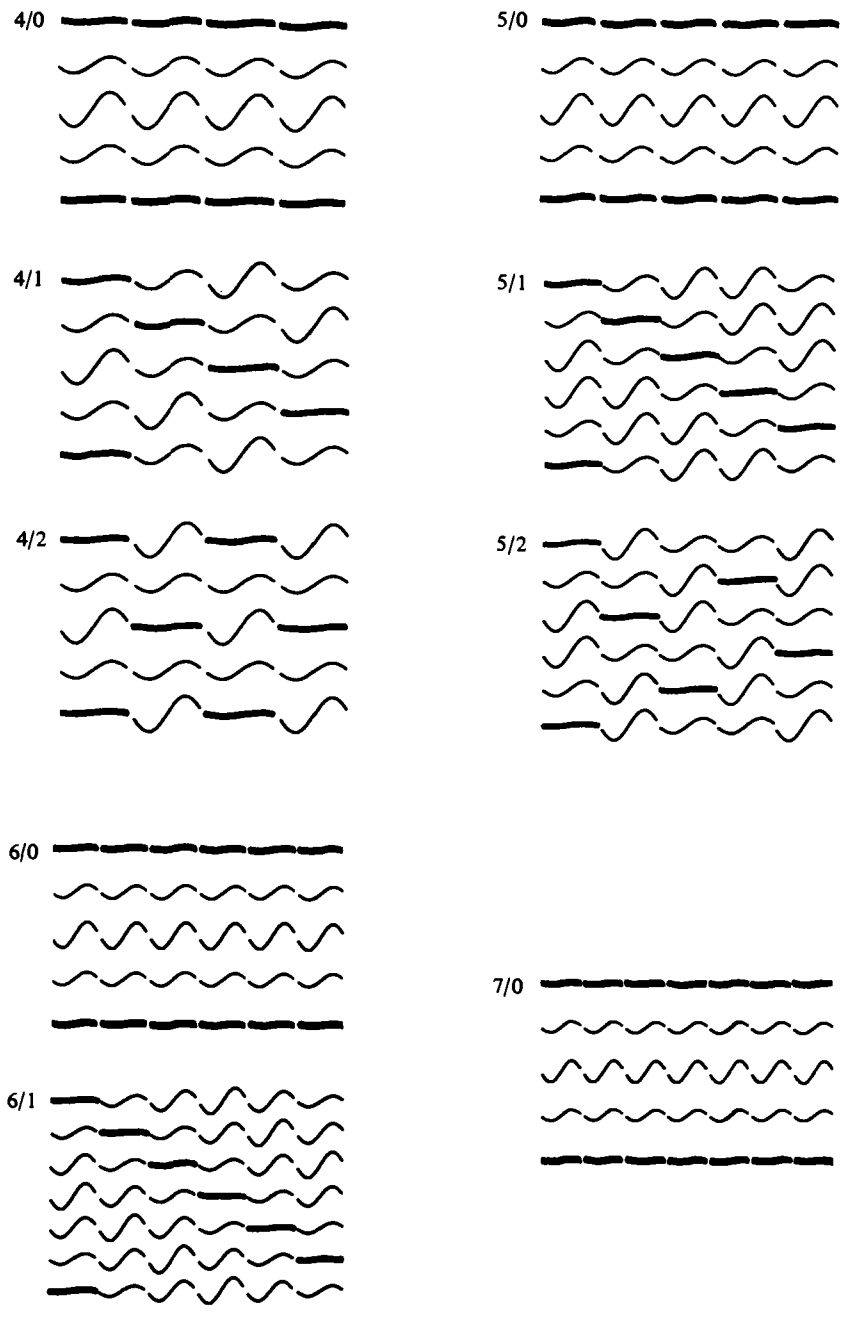

FIGURE 5. Schematic representations of the evolution in time of the modulation patterns in a reference frame rotating with the waves. The diagrams show, for each flow state pictured in figure 4, a *single* vortex outflow boundary as it evolves in time for one period of the modulation, $1/f_2'$. It should be emphasized that each diagram represents the time evolution of a single vortex boundary, not a stack of vortices at an instant of time. Time increases downward, and the azimuthal angle θ' increases (from 0 to 2π) rightward. The heavy black lines show waves that have the maximum modulation (greatest flattening).

m	k	N†	R/R_c‡	f_1	f_1/m	f_2^*	f_2'
3	0	31	19·3	1·04	0·34	0·35	0·35
4	0	16	12·6§	1·32	0·33	0·44	0·44
	1	17	10·2	1·38	0·35	0·82	0·47
	2	18	9·6	1·30	0·33	1·16	0·50
5	−1	18	15·6§	1·67	0·34	0·15	0·49
	0	17	9·6	1·72	0·34	0·51	0·51
	1	18	9·2	1·61	0·32	0·87	0·55
	2	20	12·6§	1·65	0·33	1·40	0·74
6	−1	20	10·5	2·03	0·34	0·21	0·55
	0	20	9·4	2·03	0·34	0·59	0·59
	1	19	10·2	2·05	0·34	0·99	0·65
7	0	20	8·6	2·38	0·34	0·68	0·68

† Other N values are possible for each state.

‡ The lowest observed values of R/R_c for each state. These values may differ slightly from those in figure 6 because they correspond to different N.

§ At this R/R_c there is a transition to another MWVF state at lower R/R_c.

TABLE 1. Characteristic frequencies for each MWVF state at its observed onset

MWVF has emerged from our experiments and from theory (Rand 1981; Gorman, Swinney & Rand 1981) only a few measurements are needed to determine if newly discovered states fit into this picture.

4.2. *Frequencies in doubly periodic MWVF*

The Reynolds-number dependence of the frequencies f_1 and f_2 is shown in figure 6 for nine MWVF states, and typical power spectra for those states are shown in figure 7. The values of the frequencies at the onset of MWVF are given in table 1. All frequencies in this paper are expressed in units of the cylinder frequency; the relation for conversion to Hertz is $f[\text{Hz}] = 0{\cdot}047 \times f(\text{dimensionless}) \times R/R_c$.

In the *doubly-periodic-flow* regime f_1 is independent of R within the 1% experimental uncertainty; however, the variation of f_1 (for a given m) as a function of k is as much as 3%, larger than the experimental uncertainty. Coles (1965) found that for $8 < R/R_c < 23$ the phase velocity of the wave, f_1/m, was 0·34 for all N and m. We find that $f_1/m = 0{\cdot}34 \pm 0{\cdot}01$ for all R, N, m, and k.

The frequency f_2 increases monotonically with increasing R, but the total increase over the whole MWVF region is at most 20% (see figure 6). The values of f_1 and f_2 determined from the power spectra (see figure 7) agree with those determined by flow visualization. Both the absolute and relative amplitudes of the components of the power spectra varied considerably, depending on the position of the scattering volume in the annulus, but the magnitudes of the frequencies were independent of the scattering-volume position.

Note that for the 6/0 state the upper end of the Reynolds-number range is demarked by a transition to another MWVF state rather than the disappearance of the waves (see figure 6). Similarly, for the 4/0 and 5/2 states the low end of the Reynolds-number range for each state is demarked by a transition to another MWVF state rather than a transition to WVF. However, in another system in our laboratory the 4/0 state is stable as R is decreased until it makes a transition to WVF. The difference may arise from a dependence of the stability of the 4/0 state on N or end conditions.

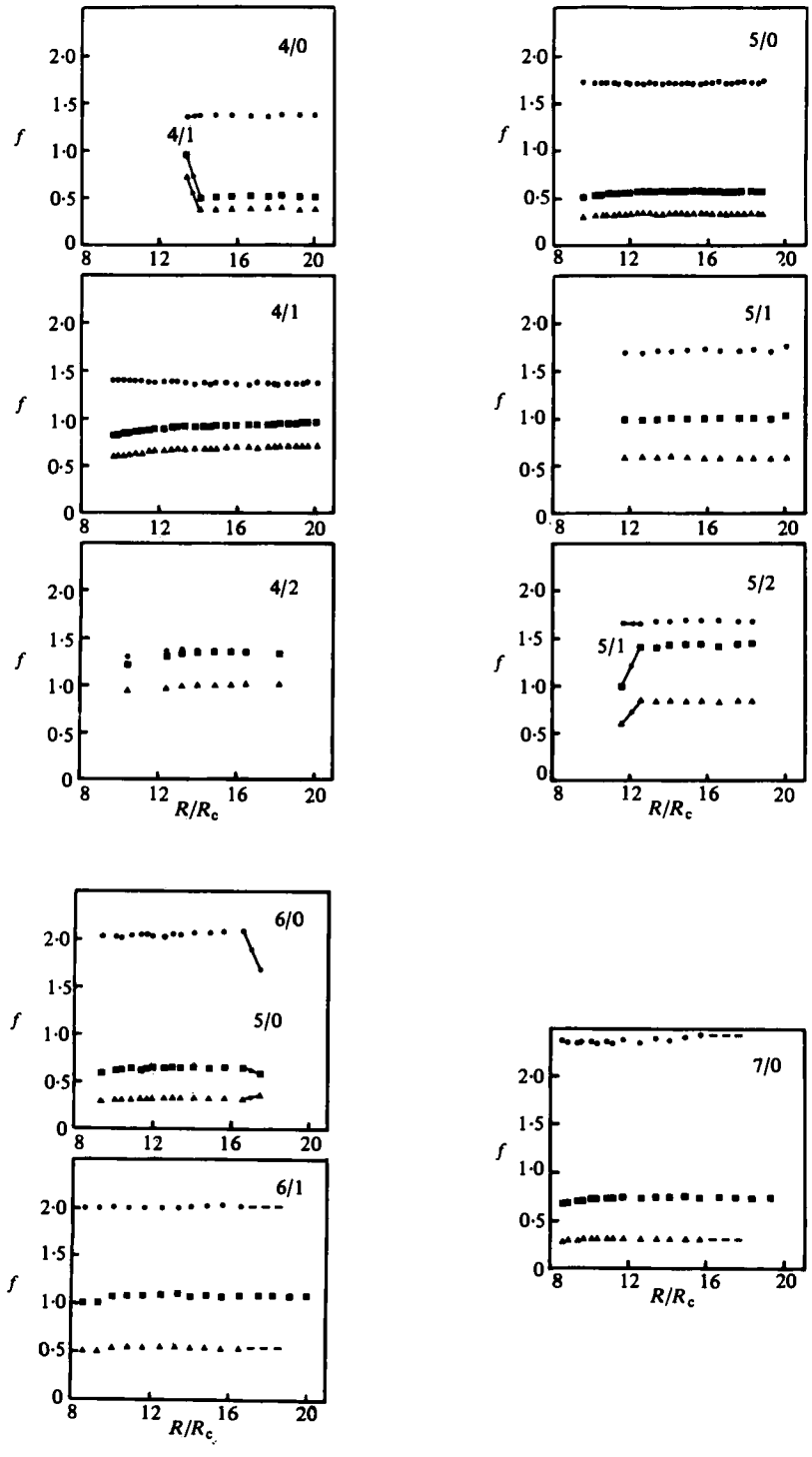

FIGURE 6. The Reynolds-number dependence of the frequency measured in flow-visualization experiments in the laboratory reference frame: ●, f_1; ■, f_2; ▲, f_3/f_1. The dashed lines indicate f_1 values too high to determine visually. Transitions from the 4/0, 5/2, and 6/0 states to other MWVF states are indicated by arrows.

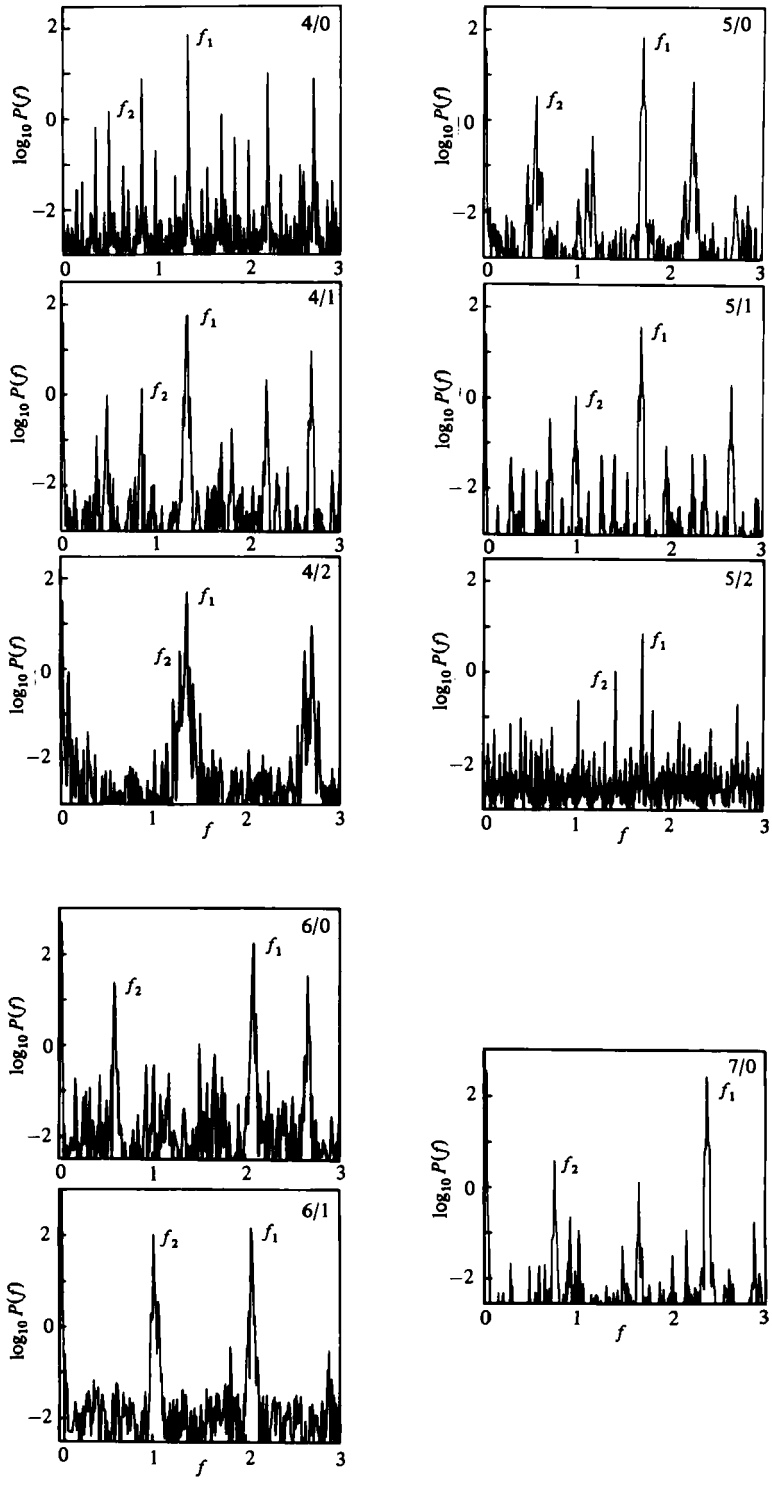

FIGURE 7. Power spectra of the intensity of light reflected by the fluid for the states described by figures 4, 5 and 6. All frequency components are integer-linear combinations of f_1 and f_2.

Previously we reported that the (doubly periodic) 5/1 state made a transition to a triply periodic state when R/R_c was reduced below $R/R_c = 12{\cdot}2$ (Gorman, Reith & Swinney 1980; Gorman *et al.* 1981). A careful re-examination of the data has shown that f_2 decreases monotonically from $f_2 = 1{\cdot}00$ at $R/R_c = 12{\cdot}2$ to $f_2 = 0{\cdot}87$ at $R/R_c = 9{\cdot}2$ (a range of R/R_c not shown for the 5/1 state in figure 6); the previously identified third independent frequency that occurs in the spectra in this range of R/R_c is actually the cylinder frequency ($f_{cyl} = 1{\cdot}00$), not a fundamental frequency of the flow. The earlier misinterpretation of the data arose because, for $R/R_c > 12{\cdot}2$, f_2 and f_{cyl} are equal.

The other frequency determined in the experiments is f_1'; values of f_2' at the onset of MWVF are given in table 1. These values of f_2' were calculated from the equation

$$f_2' = f_2 - kf_1/m, \tag{2}$$

which was derived by Swift *et al.* (1981) from a consideration of the transformation from the rotating to the laboratory frame. This equation was verified for each state by a direct comparison of f_2' measured from the ciné films at a particular R/R_c with the values of f_2' computed from the measured values of f_1 and f_2.

4.3. *Frequency modulation*

We have examined the 4/0 and 5/0 states and found that the azimuthal travelling waves are amplitude *and* frequency modulated, and the frequency of both modulations is the same $-f_2$, which for $k = 0$ is equal to f_2'.

If the phase velocity and wavelength of the azimuthal waves were both constant, the time T for successive waves to pass an observer in the laboratory would be constant. For the $m/0$ states the waves must have equal wavelength, because the wave patterns have m-fold axial symmetry. Therefore an oscillation in T would imply that the rotational frequency of the waves was frequency-modulated.

We measured T for successive waves by analysing ciné films, counting the number of film frames that passed between successive wave nodes. We measured $\overline{T}$ for 20 waves and computed $\Delta T = T - \overline{T}$ for 16 successive waves for the 5/0 state; ΔT oscillated as shown in figure 8, while for WVF ΔT was found to be zero. The solid line represents a least-squares fit of the data to a sine function, from which the amplitude of the frequency modulation, 7%, was obtained. The flattened waves have a phase velocity which is 14% slower than the S-shaped waves. The frequency modulation occurs, within the experimental uncertainty, at the same frequency as that of the amplitude modulation, f_2'. Similar results have been obtained from the frequency modulation of the 4/0 state.

We have not measured the frequency modulation for any states with $k \neq 0$, since in the absence of m-fold axial symmetry one cannot assert that all wavelengths are equal. In fact, it *appears* (from visual observations) that for $k \neq 0$ the flattened wave is stretched relative to the others, but the magnitude of the lengthening is small ($\simeq 5\%$) if present.

The presence of frequency modulation cannot be inferred directly from the components in the power spectra. For a system such as this in which the fundamental components have a strong harmonic structure, amplitude and frequency modulation can each produce the same spectral components (Gregg 1977).

The presence of frequency modulation for the $k = 0$ states has also been observed

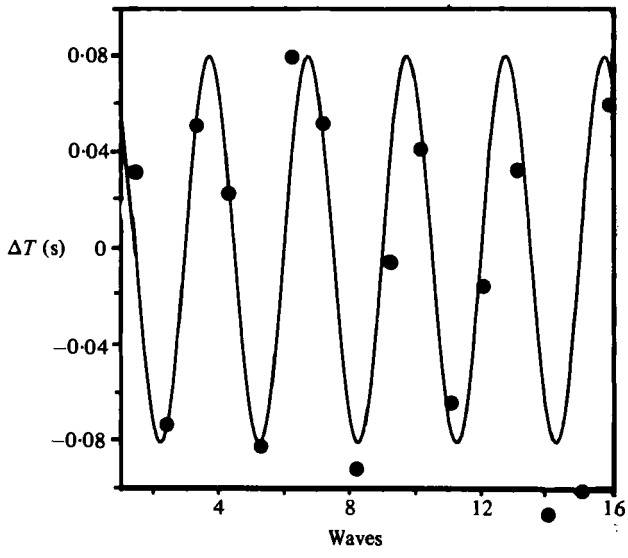

FIGURE 8. The deviation ΔT from the mean time of arrival (1·20 s) of waves as a function of the number of waves that have passed the observer (5/0 state, $R/R_c = 10{\cdot}7$).

directly by using a stroboscope to flash at the frequency f_1. In WVF the wave pattern viewed with the stroboscope was stationary, but in MWVF the waves oscillated in amplitude and in azimuthal position – the latter motion corresponds to a frequency modulation of f_1 at frequency f_2'. Thus in a frame rotating with the phase velocity of the waves, f_1/m, the waves oscillate azimuthally at f_2'; the schematic diagrams in figure 5 are made in this frame with the effects of frequency modulation neglected.

4.4. *Preparation of flow states*

Different initial conditions produce different flow states that are stable over the same range of Reynolds number. We will describe the procedures we have used to obtain the different MWVF states so they can be produced in other laboratories. If the system is started from rest and R is varied in a particular way until some final R is reached, the same state $N/m/k$ should in principle always be produced, since the system is governed by deterministic equations of motion. However, in practice our acceleration rates are not well controlled, and we observe different states for the same starting procedure.

Our procedures for obtaining different states developed from the following observations. (i) For a given N some m values are more probable than others. (ii) For a given N/m state some k values are more probable than others. (iii) If R is varied slowly in the range $6 < R/R_c < 25$, N does not usually change; this range contains the MWVF regime, $9 \lesssim R/R_c \lesssim 21$. For $N = 16$ to 19, the most probable values of m are 6 and 7. Usually even-N values occurred with a fixed upper boundary and odd-N with a free upper surface, but odd-N values were often observed with a fixed boundary and even-N with a free surface. Because the patterns do not depend on N or on the boundary conditions, the states of the flow can be labelled m/k.

Two principal procedures have been used to start the system. (*a*) The inner cylinder

was started from rest and accelerated in about one second to $R/R_c \simeq 6$, where a WVF state with $N = 15$, 16 or 17 usually formed. If the motor was shut off and restarted after a few seconds, a state with larger N usually formed. This procedure was repeated to produce any N between 15 and 21. After the desired N was achieved, R was slowly† increased until $R/R_c > 9$, where both f_2 and f_1 were present. (*b*) The desired N was obtained by procedure (*a*), and then R was slowly† increased up to $R/R_c \simeq 25$, where both f_1 and f_2 had disappeared, and finally R was decreased to $R/R_c < 21$, where both f_1 and f_2 were present.

We now describe the way in which particular m/k states were obtained. After a state was obtained, it was identified by visual measurements of f_1 and f_2.

The 6/0 and 7/0 states were obtained by procedure (*a*) with $N = 20$ or 21. The 6/1 state was obtained by procedure (*b*) with $N = 20$ or 21.

If procedure (*b*) was used with $N = 15$, then a 4/0 state usually formed, while, with $N = 16$ or 17, a 4/1 state formed more often than a 5/0 or 5/1 state; with $N = 18$ or 19, a 5/0 or 5/1 state was more likely. The 4/2 state was obtained by procedure (*b*) with $N = 18$ or 19, and the 5/2 state was obtained by procedure (*b*) with $N = 21$.

The $6/-1$ and $5/-1$ states were the most difficult to prepare. They seemed to form by using procedure (*b*) with $N = 20$ or 21 and $N = 18$ or 19, respectively; however, a rapid deceleration to $R/R_c = 16$ was substituted for a slow deceleration to $R/R_c < 21$.

The 11 states described above were all obtained for $\Gamma = 20$, but the 3/0 state was stabilized only at a larger aspect ratio. It was produced by procedure (*a*).

As an example, consider the preparation of the 4/2 state. Procedure (*a*) was used to obtain a state with $N = 18$ or 19, with any value of m. Then procedure (*b*) was followed. If a 4/0, 4/1, or $5/k$ state formed, procedure (*b*) was repeated until the 4/2 state was observed.

5. Comparison of experiment and theory

Rand (1981) has used dynamical-systems concepts and symmetry considerations to derive predictions about the space–time symmetry of doubly periodic flows in circularly symmetric systems (see also Gorman *et al.* 1981). We will summarize briefly the assumptions and predictions of the theory, and then compare theory and experiment.

Rand notes that the circular symmetry of the boundary conditions implies that the equations of motion are invariant under the group of axial rotations; therefore, following a solution from time t and then rotating that solution by θ (measured with respect to the laboratory frame) is the same as rotating the initial conditions by θ and then following the solution defined by this procedure for time t. Rand then assumes the following. (*a*) In WVF the fluid flow can be represented by an orbit in state space that is asymptotic to an attracting periodic orbit (limit cycle) consisting of non-axisymmetric states. (See Lanford (1981) for a discussion of the representation of fluid flows by attractors in state space.) (*b*) The bifurcation from WVF to MWVF is a supercritical Hopf bifurcation or some simple variant such as slightly subcritical Hopf bifurcation involving hysteresis. This assumption implies that the number of

† Here slowly means $d(R/R_c)/dt < 1\ \text{min}^{-1}$.

m	k	n	s	m	k	n	s
3	−1	−1	1	6	−2	−1	2
	0	0	3		−1	−1	1
	1	1	1		0	6	6
					1	1	1
4	−1	−1	1		2	1	2
	0	0	4		3	±1	3
	1	1	1				
	2	±1	2	7	−3	2	1
					−2	3	1
5	−2	2	1		−1	−1	1
	−1	−1	1		0	0	7
	0	0	5		1	1	1
	1	1	1		2	−3	1
	2	−2	1		3	2	1

TABLE 2. The integers from equations (1) and (3) that characterize the possible MWVF states for $m = 3, 4, 5, 6$ and 7; s is the order of the axial symmetry of the flow

waves, m, is a multiple of the order of axial symmetry of the flow, s. In MWVF the orbit is asymptotic to an attracting two-dimensional torus.

The following predictions are then derived by Rand.

(i) The wave pattern seen by an observer fixed in a reference frame rotating with the speed of the waves repeats after a basic time τ. The pattern is then the same as the original one rotated through an angle

$$\Theta = 2n\pi/m, \tag{3}$$

where Θ is measured with respect to the rotating frame and increases in the direction of the cylinder rotation, and n is an integer given by the theory. Values of n for $m = 3$ to 7 are given in table 2.

(ii) The flow is characterized by two fundamental angular frequencies

$$\Omega_1 = 2\pi s(f_1 + n/\tau)/m, \quad \Omega_2 = 2\pi/\tau. \tag{4a, b}$$

(iii) The travelling azimuthal waves are, in general, frequency-modulated as well as amplitude-modulated, and the modulation frequencies are related by $f_{\mathrm{FM}} = pf_{\mathrm{AM}}$, where p is an integer.

(iv) Frequency entrainment (where, over some range in R, Ω_1/Ω_2 is given by the ratio of small integers) occurs only if $\tau \to \infty$.

We now compare each of these predictions with the experimental observations:

(i) The prediction that the only allowed doubly periodic MWVF's are those described by (3) is in complete accord with our experiments. We have described the observed wave patterns in terms of a temporal phase angle given by (1); the *same* patterns are described in the theory in terms of an angular rotation given by (3). Thus a MWVF pattern can be characterized equivalently by either the integers m and k or by the integers m, s and n; see table 2. The time τ for the pattern to repeat, shifted by $2n\pi/m$, is related to f_2' by $\tau = s/mf_2'$, as figure 9 illustrates for a particular case.

(ii) If Ω_1 and Ω_2 are fundamentals, then any frequencies, and in particular f_1 and

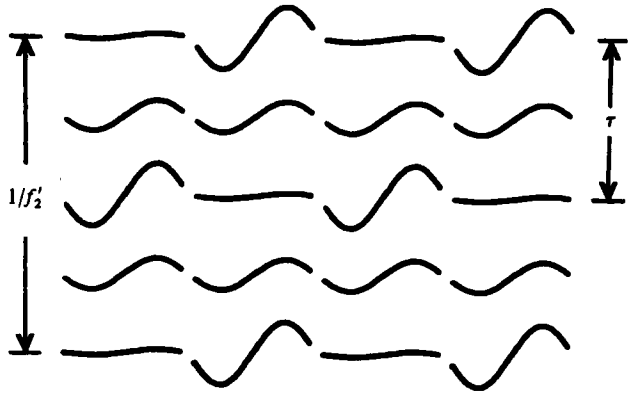

FIGURE 9. An example of the relationship between the two times measured in the reference frame that rotates with the waves: $\tau = s/mf_2'$, where f_2' is the frequency of oscillation of any point on the wave pattern, and τ is the time required for the pattern to repeat, rotated by $2n\pi/m$. The schematic diagram is of the same type as those shown in figure 5. The parameters for the example are $m = 4$, $k = 2$, $s = 2$, and $n = \pm 1$.

f_2, must be expressible as integer-linear combinations of Ω_1 and Ω_2. From (2) and (4) one obtains

$$2\pi f_1 = (m/s)\Omega_1 - n\Omega_2. \tag{5a}$$

$$2\pi f_2 = k\Omega_1 + [(s-nk)/m]\Omega_2. \tag{5b}$$

The coefficients m/s, n and k are obviously integers, and $(s-nk)/m$ is apparently always an integer (although this has not been proved); hence the prediction that Ω_1 and Ω_2 are the fundamentals is consistent with the experiments.†

(iii) As described in § 4.3, the travelling azimuthal waves have been found to be frequency-modulated, and measurements for the 4/0 and 5/0 states yield $f_{\mathrm{FM}} = f_{\mathrm{AM}}$, in agreement with the theory, where $p = 1$.

(iv) The absence of frequency entrainment is supported by the experiments: f_2/f_1 is a strictly increasing smooth function of Reynolds number for all states, as figure 6 illustrates. The experimental uncertainty in f_2/f_1 was 2% for most of our measurements, but some precision measurements on the 4/0 state in which the uncertainty in f_2/f_1 was only 0·02% revealed no evidence for entrainment.

In summary, the predictions of Rand are in accord with all of our experiments on doubly periodic MWVF.

The only other theoretical work that relates directly to our experiments is the numerical analysis by Yahata (1978, 1979, 1980) of a model with 32 coupled-mode equations. The model has one axial mode, two azimuthal modes (corresponding to $m = 0$ and $m = 4$), and eight radial modes. Using parameters appropriate to our experiments, Yahata found four successive dynamical regimes: periodic, doubly periodic, triply periodic, and chaotic.

Yahata identified two frequencies, $p_1 = 1{\cdot}5$ and $p_2 = 1{\cdot}1$, in his spectra of the doubly periodic regime, and these frequencies were compared with the frequencies $f_1 = 1{\cdot}3$ and $f_2 = 0{\cdot}9$ observed by Fenstermacher *et al.* (1979). However, our

† Note that the fundamental frequencies which characterize a power spectrum need not be present in the spectrum as observable components.

experiments have identified the state Fenstermacher *et al.* studied as the 4/1 state, which does not possess the fourfold symmetry of Yahata's model. His calculations are more appropriate to the fourfold-symmetric 4/0 state for which $f_1 = 1{\cdot}3$ and $f_2 = 0{\cdot}4$. Yahata could also have chosen as fundamental frequencies his spectral components at 1·5 and 0·4, which are in good agreement with the measured frequencies for the 4/0 state. The experimental results for the 5/0, 6/0, and 7/0 states provide a test for this model.

The triply periodic state found for the model appeared at $R/R_c = 20{\cdot}7$ and existed up to $R/R_c = 22{\cdot}7$, beyond which the flow was chaotic. We have found no triply periodic states.

6. Discussion

6.1. *Circularly symmetric systems*

All of the results reported here have been obtained with a radius ratio of 0·88. Time-dependent flows in the circular Couette system have been studied for radius ratios other than 0·88 (see Snyder 1970; Kuznetsov *et al.* 1980; Pfister 1981), but the existence of MWVF for $\eta \neq 0{\cdot}88$ has not yet been established.

Travelling azimuthal waves which periodically change their shape have been studied in another circularly symmetric flow geometry, a rotating annulus with a temperature gradient applied in the radial direction. Hide (1953, 1958) discovered that, for some range of the rotation rate and radial temperature gradient, travelling azimuthal waves were observed in the annulus, and in another parameter range a 'vacillation' in the shape of the travelling waves was observed. Shape vacillation was also studied by Fultz *et al.* (1959), and later Pfeffer & Chiang (1967) observed another type of vacillation, amplitude vacillation, as well as shape vacillation. Shape and amplitude vacillation have subsequently been studied by Pfeffer & Fowlis (1968), Hide & Mason (1975), Pfeffer, Buzyna & Kung (1980), White & Koschmieder (1981) and others. Only White & Koschmieder have obtained power spectra and have shown that the vacillating flow is a doubly periodic flow.

Pfeffer & Fowlis (1968) illustrated amplitude vacillation with figures showing time-lapsed sequences of the flow patterns. The flows shown in their figures appear to have the same space–time symmetry as some of the states we have observed. For example, their figure 5 appears to be a 4/0 state; figure 6, 5/0; and figure 11, 5/ − 1. They show that these states can be viewed as a superposition of travelling azimuthal waves, each with its own wave speed and wavenumber. Robert Shaw (private communication) has independently suggested that a picture of superimposed travelling waves could describe the doubly periodic flows we have observed; Shaw and the authors are now testing this hypothesis.

Vacillation in the rotating annulus was studied theoretically by Lorenz (1963*b*), who developed a model consisting of 14 coupled nonlinear ordinary differential equations. Solutions for the travelling azimuthal waves were obtained analytically. Solutions exhibiting vacillation were obtained by numerical integration, and Lorenz even found non-periodic solutions beyond the vacillation regime. The sequence of regimes described by Lorenz is quite similar to the sequence we have observed in the Couette system.

Another cylindrically symmetric flow geometry that has been extensively studied

is a fluid contained between concentric spheres with one or both spheres rotating (Sawatzki & Zierep 1970; Munson & Menguturk, 1975; Wimmer 1976, 1981; Yavorskaya *et al.* 1981; Belyaev *et al.* 1979). Complex wavy flows have been observed in this system, but, to our knowledge, modulated (vacillating) waveforms have not been reported.

6.2. *Conclusions*

We have shown that the circular Couette system exhibits a multiplicity of doubly periodic modulated wavy-vortex flow states, each characterized by two integers, m and k, which have a simple physical significance. Using different initial conditions, we have discovered twelve different stable states m/k during our two-year study. Other stable states can undoubtedly be reached with other initial conditions; in retrospect it is surprising that only the 4/1 state was observed in the first four years of study of doubly periodic flow in the Couette system (Gollub & Swinney 1975; Fenstermacher *et al.* 1979; Walden & Donnelly 1979).

Ruelle (1973) suggested that symmetry properties could restrict the types of bifurcations that can occur in hydrodynamic systems. The theory of Rand (1981) is the first to use symmetry to obtain specific predictions about the dynamics of flows in systems with a particular symmetry. As we have shown in § 5, Rand's predictions are in good agreement with our experiments.

Rand's theory applies to doubly periodic flows in circularly symmetric systems which satisfy the assumptions stated in § 5. However, it should be noted that some circularly symmetric systems may have doubly periodic flows that do not satisfy all of those assumptions and hence the predictions (i) – (iv) would not apply.

Fenstermacher *et al.* (1979) studied the transition from doubly periodic flow to weak turbulence for the 4/1 state, but this transition has not been studied for any of the other 11 observed doubly periodic flow states. Ws are making a comparative study of the onset of turbulence in the different states with the hope that such a study will provide insight into the transition-to-turbulence problem.

This work is supported by National Science Foundation Grant CME 79–09585. We acknowledge helpful discussions with Jack Swift, W. D. McCormick, E. L. Koschmieder, and Robert Shaw. We thank Gregory King and Ken Mednick for assistance in computer programming; Leslie Reith and David Andereck for assistance in the experiments; and Truett Majors and Karl Trappe for assistance with the photographic work. We especially thank David McWilliams and Fred Akers of the University of Texas Athletic Department for the use of the projector that enabled us to analyse the ciné films frame by frame.

REFERENCES

BELYAEV, YU. N., MONAKOV, A. A., SHERBAKOV, S. A. & YAVORSKAYA, I. M. 1979 *JETP Lett.* **29**, 329.

BENJAMIN, T. B. 1978 *Proc. R. Soc. Lond.* A **359**, 27.

BOUABDALLAH, A. & COGNET, G. 1980 Laminar–turbulent transition in Taylor–Couette flow. In *Laminar–Turbulent Transition* (ed. R. Eppler & H. Fasel), p. 368. Springer.

COLES, D. 1965 *J. Fluid Mech.* **21**, 385.

DIPRIMA, R. C. & SWINNEY, H. L. 1981 Instabilities and transition in flow between concentric rotating cylinders. In *Hydrodynamic Instabilities and the Transition to Turbulence* (ed. H. L. Swinney & J. P. Gollub), p. 139. Springer.

DONNELLY, R. J., PARK, K., SHAW, R. & WALDEN, R. W. 1980 *Phys. Rev. Lett.* **44**, 987.

FENSTERMACHER, P. R., SWINNEY, H. L. & GOLLUB, J. P. 1979 *J. Fluid Mech.* **94**, 103.

FULTZ, D., LONG, R. R., OWENS, G. V., BOHAN, W., KAYLOR, R. & WEIL, J. 1959 *Met. Monographs* **4**, 1.

GOLLUB, J. P. & SWINNEY, H. L. 1975 *Phys. Rev. Lett.* **35**, 927.

GORMAN, M., REITH, L. & SWINNEY, H. L. 1980 *Ann. N.Y. Acad. Sci.* **357**, 10.

GORMAN, M. & SWINNEY, H. L. 1979 *Phys. Rev. Lett.* **43**, 1871.

GORMAN, M., SWINNEY, H. L. & RAND, D. 1981 *Phys. Rev. Lett.* **46**, 992.

GREGG, W. D. 1977 *Analog and Digital Communication.* Wiley.

HIDE, R. 1953 *Quart. J. R. Met. Soc.* **79**, 161.

HIDE, R. 1958 *Phil. Trans. R. Soc. Lond.* A **250**, 441.

HIDE, R. & MASON, P. J. 1975 *Adv. Phys.* **24**, 47.

KUZNETSOV, E. A., LVOV, V. S., PREDTECHENSKII, V. S., SOBOLEV, V. S. & UTKIN, E. N. 1980 *Sov. Phys. JETP Lett.* **30**, 207.

LANFORD, O. E. 1981 Strange attractors and turbulence. In *Hydrodynamic Instabilities and the Transition to Turbulence* (ed. H. L. Swinney & J. P. Gollub), p. 7. Springer.

LORENZ, E. N. 1963*a* *J. Atmos. Sci.* **20**, 130.

LORENZ, E. N. 1963*b* *J. Atmos. Sci.* **20**, 448.

MOBBS, F. R., PRESTON, S. & OZOGAN, M. S. 1979 An experimental investigation of Taylor vortex waves. In *Taylor Vortex Flow Working Party, Leeds*, p. 53.

MUNSON, B. R. & MENGUTURK, M. 1975 *J. Fluid Mech.* **69**, 705.

PFEFFER, R. L., BUZYNA, G. & KUNG, R. 1980 *J. Atmos. Sci.* **37**, 2129.

PFEFFER, R. L. & CHIANG, Y. 1967 *Mon. Weather Rev.* **95**, 75.

PFEFFER, R. L. & FOWLIS, W. W. 1968 *J. Atmos. Sci.* **25**, 361.

PFISTER, G. & GERDTS, U. 1981 *Phys. Lett.* **83A**, 23.

RAND, D. 1981 *Arch. Rat. Mech. Anal.* (to appear).

RUELLE, D. 1973 *Arch. Rat. Mech. Anal.* **51**, 136.

RUELLE, D. & TAKENS, F. 1971 *Commun. Math. Phys.* **20**, 167.

SAWATZKI, O. & ZIEREP, J. 1970 *Acta Mech.* **9**, 13.

SNYDER, H. A. 1970 *Int. J. Nonlinear Mech.* **5**, 659.

SWIFT, J., GORMAN, M. & SWINNEY, H. L. 1981 *Phys. Lett.* (to appear).

TAYLOR, G. I. 1923 *Phil. Trans. R. Soc. Lond.* A **223**, 289.

WALDEN, R. & DONNELLY, R. J. 1979 *Phys. Rev. Lett.* **42**, 301.

WHITE, D. & KOSCHMIEDER, E. L. 1981 *Geophys. Astrophys. Fluid Dyn.* **18**, 301.

WIMMER, M. 1976 *J. Fluid Mech.* **78**, 317.

WIMMER, M. 1981 *J. Fluid Mech.* **103**, 117.

YAHATA, H. 1978 *Prog. Theor. Phys. Suppl.* **64**, 176.

YAHATA, H. 1979 *Prog. Theor. Phys.* **61**, 791.

YAHATA, H. 1980 *Prog. Theor. Phys.* **64**, 782.

YAVORSKAYA, I. M., BELYAEV, YU. N., MONAKHVO, A. A., ASTAF'EVA, N. M., SCHERBAKOV, S. A. & VREDENSKAYA, N. D. 1981 (to be published).